Psychoradiology, 2022, **2**, 190–198
DOI: 10.1093/psyrad/kkac023
Advance access publication date: 15 December 2022
Research Article

Structural covariance network of the hippocampus–amygdala complex in medication-naïve patients with first-episode major depressive disorder

Lianqing Zhang [1,#], Xinyue Hu [2,#], Yongbo Hu [3], Mengyue Tang [1], Hui Qiu [2], Ziyu Zhu [1], Yingxue Gao [1], Hailong Li [1], Weihong Kuang [3,*] and Weidong Ji [4,5,*]

[1]Functional and molecular imaging Key Laboratory of Sichuan Province, West China Hospital, Sichuan University, Chengdu 610041, PR China
[2]Department of Radiology, West China Hospital of Sichuan University, Chengdu 610041, PR China
[3]Department of Psychiatry, West China Hospital of Sichuan University, Chengdu 610041, PR China
[4]Shanghai Key Laboratory of Mental Health and Psychological Crisis Intervention, School of Psychology and Cognitive Science and Affiliated Mental Health Center, East China Normal University, Shanghai 200335, China
[5]Child Psychiatry, Shanghai Changning Mental Health Center, Shanghai 200335, China
*Correspondence: Weihong Kuang, kwhhlj@163.com; Weidong Ji, wdji@psy.ecnu.edu.cn
[#]Lianqing Zhang and Xinyue Hu Contribute equally to this work.

Abstract

Background The hippocampus and amygdala are densely interconnected structures that work together in multiple affective and cognitive processes that are important to the etiology of major depressive disorder (MDD). Each of these structures consists of several heterogeneous subfields. We aim to explore the topologic properties of the volume-based intrinsic network within the hippocampus–amygdala complex in medication-naïve patients with first-episode MDD.

Methods High-resolution T1-weighted magnetic resonance imaging scans were acquired from 123 first-episode, medication-naïve, and noncomorbid MDD patients and 81 age-, sex-, and education level-matched healthy control participants (HCs). The structural covariance network (SCN) was constructed for each group using the volumes of the hippocampal subfields and amygdala subregions; the weights of the edges were defined by the partial correlation coefficients between each pair of subfields/subregions, controlled for age, sex, education level, and intracranial volume. The global and nodal graph metrics were calculated and compared between groups.

Results Compared with HCs, the SCN within the hippocampus–amygdala complex in patients with MDD showed a shortened mean characteristic path length, reduced modularity, and reduced small-worldness index. At the nodal level, the left hippocampal tail showed increased measures of centrality, segregation, and integration, while nodes in the left amygdala showed decreased measures of centrality, segregation, and integration in patients with MDD compared with HCs.

Conclusion Our results provide the first evidence of atypical topologic characteristics within the hippocampus–amygdala complex in patients with MDD using structure network analysis. It provides more delineate mechanism of those two structures that underlying neuropathologic process in MDD.

Keywords: Major depressive disorder; hippocampus–amygdala complex; structural covariance network; global network metrics; local network metrics

Introduction

Major depressive disorder (MDD) is one of the most prevalent, debilitating affective disorders and is characterized by depressed mood, diminished interest, impaired cognitive function, and vegetative symptoms (Otte *et al.*, 2016). Psychoradiological evidence accumulated in recent decades has emphasized the importance of the hippocampus and the amygdala in the neuropathology of MDD (Chen *et al.*, 2021). The hippocampus and amygdala are heavily interconnected structures that subserve integrated cognitive and affective functions; in this capacity, they are commonly referred to as the hippocampus–amygdala complex (Fudge *et al.*, 2012; Terranova *et al.*, 2022). The Enhancing Neuroimaging Genetics through Meta-Analysis (ENIGMA) MDD working group detected significantly lower overall hippocampal volumes in MDD patients than in healthy control (HC) participants, especially in patients with recurrent MDD or with an early age of onset (Schmaal *et al.*, 2016). While multi-site studies with large sample size found no differences in the whole amygdala volume, several single-site studies with clinically homogeneous samples found an overall decrease in amygdala volume in patients with MDD (Zavorotnyy *et al.*, 2018; Weissman *et al.*, 2020; Kim *et al.*, 2021).

Since both of the hippocampus and amygdala consist of histologically and functionally heterogeneous subfields/subregions, apart from total volumes of these structures, studies have shown selective alterations in hippocampal subfields and amygdala subregions in relation to MDD (Boll *et al.*, 2013; Iglesias *et al.*, 2015; Whelan *et al.*, 2016). The ENIGMA working group also reported that patients with MDD had reduced thickness and surface area in the subiculum and CA2/3 areas of the hippocampus and basolateral amygdala, and these effects were primarily driven by MDD with an adolescent age of onset (Ho *et al.*, 2022). Recurrence of MDD was associated with reduced surface area and thickness in the

Received: 4 November 2022; **Revised:** 5 December 2022; **Accepted:** 14 December 2022

basolateral amygdala and in the CA1 region of the hippocampus (Ho *et al.*, 2022). Our previous study reported a larger bilateral subiculum, CA1 and left CA2/3, CA4/dentate gyrus (DG) in MDD patients who did not show an early effective response to antidepressants than in HCs or patients with an early treatment response (Hu *et al.*, 2019). Regional amygdala volume alterations were also reported (Yao *et al.*, 2020; Kim *et al.*, 2021; Roddy *et al.*, 2021).

These reports point that multiple but no single subfields of the hippocampus and subregions of the amygdala were affected in MDD. However, it remains unknown whether volume alterations in these subfields or subregions in the hippocampus–amygdala complex can be described with higher, network-level patterns, and whether these patterns would be atypical in patients with depression. Indeed, a number of studies found covariation in morphology of different brain areas (structural covariance) showed network properties and were atypical in patients with MDD, but all of them reported whole-brain structural covariance abnormalities and no study to date has focused on the structural covariance network (SCN) within the hippocampus–amygdala complex (Yee *et al.*, 2018; Watanabe *et al.*, 2020; Li *et al.*, 2021; Xiong *et al.*, 2021). Although the neurobiology meaning of the SCN was yet to be known, some have studies pointed to common neural substrates that influence multiple brain regions simultaneously—genetic and environmental factors that influences trajectories in brain development and maturation, or continuously reshaping the brain during the lifespan (Zielinski *et al.*, 2010; Yee *et al.*, 2018; Qi *et al.*, 2019; Plachti *et al.*, 2020). Interestingly, SCN were found similar to patterns of functional connectivity than the architecture of white matter connections, and graph theory metrics were commonly used to describe the characteristics of SCN in psychoradiology studies (Yun *et al.*, 2020). Studies on atypical SCN in psychiatric disorders are important as they provide clues for future studies to find underlying neural substrates or subserve as a candidate for transdiagnosis biomarkers (Liu *et al.*, 2021; Han *et al.*, 2022) (Li *et al.*, 2015; Yun *et al.*, 2020).

In the current study, we recruited a relatively large sample of first-episode, medication-naïve, and noncomorbid patients with MDD to build a SCN based on the volumes of hippocampal subfields and amygdala subregions. We aimed to identify MDD-related covariance patterns in the localized SCN within the hippocampus–amygdala complex, which would shed light on common neural substrates that influence multiple sites in the complex.

Method

Participants

This study was approved by the Research Ethics Committee of Sichuan University, and written informed consent was obtained from all participants. We recruited 123 first-episode, medication-naïve MDD patients and 81 age- and sex-matched HCs for the present study. All participants were recruited consecutively from the outpatient or inpatient psychiatric units of local hospitals. The diagnosis of first-episode depression was made according to the Structured Clinical Interview for the DSM-IV. Acute illness severity was assessed using the 17-item Hamilton Rating Scale for Depression (HAMD) and the 14-item Hamilton Rating Scale for Anxiety (HAMA).

The inclusion criteria for patients were as follows: (i) medication-naïve with no previous episodes of depression and (ii) currently experiencing an episode of depression with a HAMD total score ≥18. The exclusion criteria included the following: (i) presence of other Axis I psychiatric disorders, including anxiety disorders, obsessive compulsive disorder, and substance use disorders (excluding nicotine); (ii) history of neurological or cardiovascular disease; (iii) pregnancy or systemic physical illness; and (iv) any contraindication to magnetic resonance imaging (MRI).

HC participants were screened for a current or lifetime history of Axis I mental disorder using the Structured Clinical Interview for the DSM-IV. Neurological and other medical disorders were identified based on personal histories and physical examinations. None of the participants had any gross neuroanatomic abnormalities or image distortion related to head motion evident on T1-weighted scans reviewed by two experienced neuroradiologists.

MRI data acquisition and processing

High-resolution T1-weighted images were obtained using a magnetization-prepared rapid gradient-echo sequence (TR/TE = 1900/2.2 ms; inversion time = 900 ms; flip angle = 9°) via a 3.0-T MRI system (Trio, Siemens, Erlangen, Germany). The matrix (256 × 256), the field of view (256 × 256 mm), and the section thickness (1 mm) together yielded an isotropic voxel size of 1 mm^3. Foam padding and earplugs were used to reduce head motion and scanner noise.

Images were automatically preprocessed using FreeSurfer software (v.6.0) (http://surfer.nmr.mgh.harvard.edu/) with the standard recon-all process. Briefly, T1-weighted images were transformed into Talairach space, and signal intensity normalization and skull-stripping procedures were performed (Sled *et al.*, 1998; Fischl *et al.*, 2002; Reuter *et al.*, 2010; Whelan *et al.*, 2016). A measurement of intracranial volume (ICV) was extracted.

The segmentation of hippocampal subfields and amygdala subregions was performed using a special module in FreeSurfer that employs a tetrahedral mesh-based probabilistic atlas built from manually delineated hippocampus and amygdala maps based on *in vivo* and *ex vivo* data (Iglesias *et al.*, 2015; Saygin *et al.*, 2017). Using this algorithm, nine subregions in the amygdala were obtained, comprising seven nuclei [lateral nucleus (La), basal nucleus (Ba), accessory basal nucleus (AB), CeA, medial nucleus (Me), cortical nucleus (Co) and paralaminar nucleus] and two transition areas [anterior amygdaloid area (AAA) and corticoamygdaloid transition area (CAT)]. Additionally, 12 subfields in the hippocampus were obtained, including the CA1, the CA3 (which contains the CA2), the CA4, the molecular and granule cell layers of the dentate gyrus, the molecular layer, the subiculum, the presubiculum, the parasubiculum, the fimbria, the fissure, hippocampal-amygdala transition area, and the tail. An example of the segmentation for a healthy participant is shown in Fig. 1. All segmentations were visually inspected according to the ENIGMA control protocol (http://enigma.ini.usc.edu/). In brief, the segmentation of each participant was independently visually checked by two coauthors (L.Z. and X.H.), and participants with segmentation results judged to be incorrect (e.g. most of the hippocampus/amygdala was cut off, or the mask was shifted with respect to the structure) were excluded. None of the participants showed segmentation failure.

Analysis of the intrinsic hippocampus–amygdala complex global and local networks

We performed a volume-based analysis of the intrinsic hippocampus–amygdala complex network with Brain Analysis using Graph Theory (BRAPH; v.1.00; http://braph.org/) (Mijalkov *et al.*, 2017). Networks were built for each group as collections

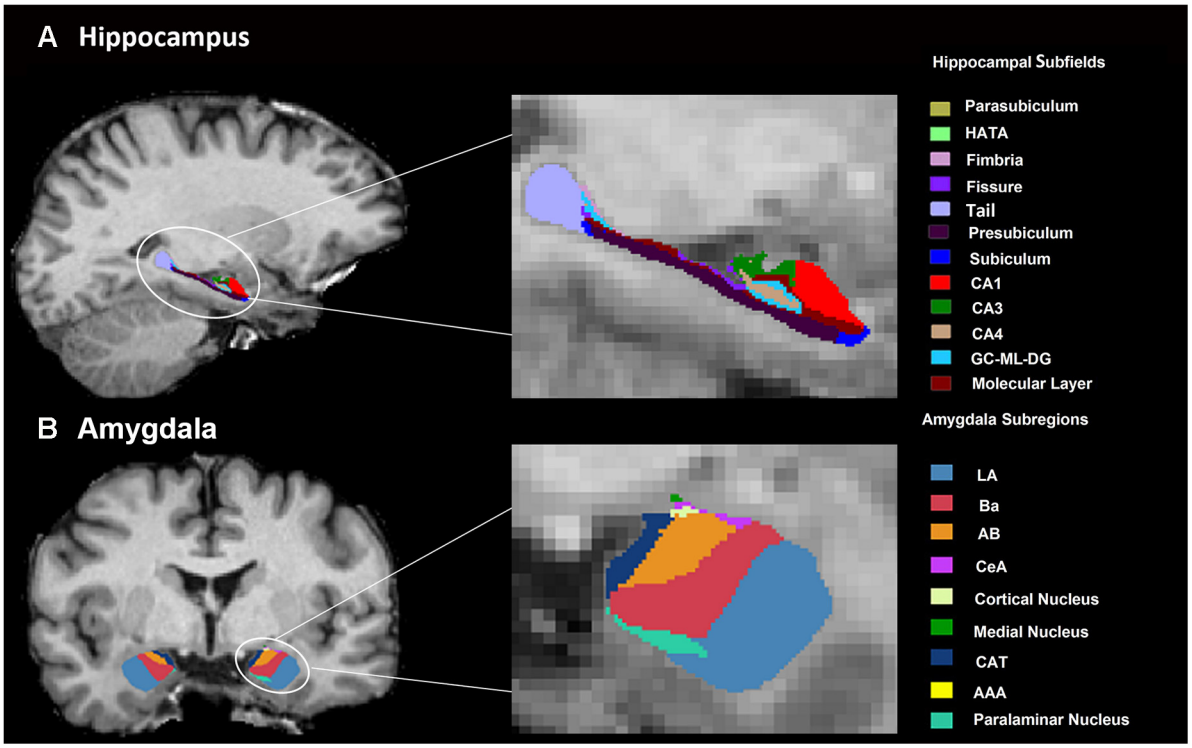

Figure 1: An example of amygdala (A) and hippocampal (B) segmentation in a healthy participant. Abbreviations: CeA, central nucleus; HATA, hippocampus–amygdala transition area; GC-ML-DG, granule cell and molecular layers of the dentate gyrus; CA, cornu ammonis.

of nodes representing individual volumes of the hippocampal subfields and amygdala subregions connected by edges corresponding to the interconnections. We used the volumes of the 18 subregions of the amygdala and the 24 subfields of the hippocampus. The edges were calculated as the partial correlation coefficients between each pair of subfields while controlling for the effects of age, sex, education level, and ICV. A structurally weighted, undirected connectivity matrix was built for each group.

Measures of brain networks

To determine the differences between groups in the intrinsic global hippocampus–amygdala complex network, we calculated graphical metrics that reflect network segregation, integration, network resilience, and centrality for the whole network and for each node, while Supplementary Table S1 contains mathematical definitions of all topological metrics. The small-worldness index is defined as the normalized clustering coefficient/characteristic path length (Bassett and Bullmore, 2006). When the minimum density of the small-worldness index is >1, a network is considered to have small-world organization (Amaral *et al.*, 2000).

Measures of segregation include clustering coefficient, transitivity, local efficiency, strength and modularity. The clustering coefficient is defined as the fraction of triangles around an individual node (Watts and Strogatz, 1998). The nodal clustering coefficient is defined as the fraction of triangles present around a node (Watts and Strogatz, 1998). Transitivity is defined as the ratio of the total number of triangles to the number of (unordered) triplets in the graph (Newman, 2003). Local efficiency is defined as the average of the local efficiencies of all nodes (Latora and Marchiori, 2001). Nodal local efficiency is defined as the global efficiency of a node calculated on the subgraph formed by the neighbors of the node (Latora and Marchiori, 2001). Strength is defined as the average of the strengths of all nodes (Rubinov and Sporns, 2010). Nodal strength is defined as the sum of the weights of all edges connected to a node (Barrat *et al.*, 2004). Modularity is defined as the extent to which a graph can be divided into clearly separated communities (Newman, 2006).

Measures of integration include characteristic path length, global efficiency, and triangles. The characteristic path length is defined as the average shortest path length between all pairs of nodes in Network (Watts and Strogatz, 1998). Global efficiency is defined as the average inverse shortest path length (Latora and Marchiori, 2001). Nodal global efficiency is defined as the average of the inverse shortest path length from a node to all other nodes (Latora and Marchiori, 2001). A triangle is defined as being present when two neighbors of a node are also neighbors to each other (Onnela *et al.*, 2005).

Resilience of the network can be measured by the assortativity coefficient. The assortativity coefficient is the correlation coefficient between the degrees of all nodes on two opposite ends of a link (Newman, 2002).

Measures of centrality include degree, average eccentricity, betweenness centrality, and closeness centrality. Degree is defined as the average of the degrees of all nodes (Rubinov and Sporns, 2010). Nodal degree is defined as the total number of edges connected to a node (Achard and Bullmore, 2007). Eccentricity is defined as the average of the eccentricities of all nodes (Harris *et al.*, 2008). Betweenness centrality is defined as the fraction of all shortest paths in the network that pass through a given node (Brandes, 2001). Closeness centrality is defined as the inverse of the average shortest path length from one node to all other nodes in the network (Freeman, 1978).

Statistical analysis

Statistical analysis of demographic data was conducted using the Statistical Package for the Social Sciences (v.19.0) software. Differences between the MDD and HC groups were examined using a two-sample t-test for continuous variables and a chi-square test for categorical variables.

The global and local hippocampus–amygdala complex network measures were compared on the network sparsity of 50% by testing the statistical significance of the differences using nonparametric permutation tests with 1000 permutations. Then, we calculated abnormal global metrics at different sparsity thresholds (20–50%, at intervals of 5%) between groups to explore how thresholds influence the results. A false discovery rate (FDR) correction was applied to correct for multiple comparisons in the analysis of the intrinsic local hippocampus–amygdala complex network.

Results

Demographic and clinical features

The demographic and clinical features of the 123 treatment-naïve individuals with MDD and 81 HCs are presented in Table 1. There were no significant differences between patients with MDD and HCs in terms of age, sex, education level, or ICV. In the patients with MDD, the mean HAMD and HAMA scores were 25.8 and 24.5, respectively.

The global topological characteristics of the intrinsic hippocampus–amygdala complex network

There were significant differences in the global network between patients with MDD and HCs (Table 2). The small-worldness index was significantly increased in patients with MDD compared to HCs (0.924 vs. 0.747, $P < 0.001$). However, the small-worldness index in both groups was <1, suggesting that the hippocampus–amygdala complex network in both the MDD and HC groups failed to present small-world organization.

The modularity was significantly decreased in patients with MDD compared to HCs (0.046 vs. 0.136, $P = 0.004$), while most measures of segregation (including average strength, local efficiency, mean clustering coefficient, and transitivity) were slightly increased in patients with MDD compared to HCs. The characteristic path length (a measure of integration) was significantly decreased in patients with MDD compared to HCs (2.721 vs. 3.490, $P = 0.029$). No significant differences were found in measures of centrality between groups. As shown in Fig. 2, alterations of index for the small-worldness, modularity, and characteristic path length remained the same trend between groups.

The nodal topological characteristics of the intrinsic hippocampus–amygdala complex network

Significant differences in local networks were mainly found in multiple subregions in the left amygdala and left hippocampal tail between patients with MDD and HCs (Fig. 3, see Supplementary Tables S2–S10 for details on the full group comparison of local network measures).

Measures of segregation

The nodal clustering coefficients of the left CAT, La, Ba, and paralaminar nucleus were significantly decreased in patients with MDD compared to HCs (FDR-corrected $P < 0.05$), while the nodal clustering coefficient of the left hippocampal tail was significantly increased in patients with MDD compared to HCs (FDR-corrected $P < 0.05$). The nodal local efficiency of the left hippocampal tail was significantly increased in patients with MDD compared to HCs (FDR-corrected $P < 0.05$). Moreover, the nodal strength of the left CAT, AB, La, Me, right fissure, and molecular layer were significantly decreased in patients with MDD compared to HCs (FDR-corrected $P < 0.05$), while the nodal strength of the left CA4 was significantly increased in patients with MDD compared to HCs (FDR-corrected $P < 0.05$).

Measures of integration

The nodal global efficiency of the left CAT, Ba, AB, AAA, and paralaminar nucleus was significantly decreased in patients with MDD compared to HCs (FDR-corrected $P < 0.05$), while the nodal global efficiency of the left hippocampal tail was significantly increased in patients with MDD compared to HCs (FDR-corrected $P < 0.05$). The nodal path length of the left CAT, Ba, and La was significantly increased in patients with MDD compared to HCs (FDR-corrected $P < 0.05$). Moreover, the triangles of the left CAT, La, AB, Ba, and paralaminar nuclei were significantly decreased in patients with MDD compared to HCs (FDR-corrected $P < 0.05$).

Measures of centrality

The betweenness centrality of the left Co was significantly increased in patients with MDD compared to HCs (FDR-corrected $P < 0.05$), while the closeness centrality of the left CAT, La, Ba, AB, AAA, and paralaminar nucleus were significantly decreased in patients with MDD compared to HCs (FDR-corrected $P < 0.05$). Moreover, the nodal degrees of the left CAT, La, parasubiculum, and presubiculum were significantly decreased in patients with MDD compared to HCs (FDR-corrected $P < 0.05$).

Discussion

In the current study, with a relatively large sample of first-episode, never-treated patients with MDD, we demonstrated for the first time the alterations of topological properties for the SCN in the hippocampus–amygdala complex in this population. Patients with MDD showed decreased characteristic path length, modularity, and small-worldness, suggesting higher network integration within the hippocampus–amygdala complex in patients than in HCs. The left hippocampal tail showed higher centrality, while nodes within the left amygdala showed lower centrality except for the left cortical nucleus of the amygdala. These findings add to previous work that reported MDD-related subregional-level neuroanatomical alterations in the hippocampus and amygdala, and highlighted potential common neural substrates underlying MDD influence multiple sites in the hippocampus–amygdala complex simultaneously.

Interestingly, we found that patients with MDD had higher network integration (as suggested by decreased characteristic path length) and lowered functional segregation (as suggested by decreased modularity) within the hippocampus–amygdala complex, as compared with HCs. Findings from whole-brain network organization studies commonly suggest increased or comparable characteristic path length (Ye *et al.*, 2015; Liu *et al.*, 2020; Yu *et al.*, 2020), and higher modularity of brain networks in patients with MDD than in HCs (Chen *et al.*, 2017). Our findings suggest that the pattern of structural network organization within the hippocampus–amygdala complex is distinct from the pattern of global network organization in MDD.

Table 1: Demographic: and clinical features of the treatment-naïve patients with MDD and HCs.

	MDD (N = 123)	HC (N = 81)	P values
Age (years)	32.4 (11.3)	33.6 (10.8)	0.440
Sex (female/male)	78/45	51/30	0.948
ICV (cm^3)	1476.8 (139.2)	1470.5 (131.2)	0.742
Age of onset (years)	30.8 (11.5)	NA	-
Illness duration (weeks)	29.7 (28.8)	NA	-
HAMD score	25.8 (5.4)	NA	-
HAMA score	24.5 (9.1)	NA	-

Notes: Data are presented as the means (standard deviation). Abbreviation: NA, not applicable.

Table 2: Differences: in the intrinsic hippocampus–amygdala global network between patients with MDD and healthy controls.

Measures	Patients with MDD	HCs	Differences	CI lower	CI upper	P value
Small-worldness index	0.924	0.747	−0.177	−0.066	0.054	**<0.001*** **
Measures of segregation						
Average strength	16.964	13.997	−2.967	−3.727	3.865	0.244
Local efficiency	1.262	1.043	−0.218	−0.365	0.441	0.405
Mean clustering coefficient	0.394	0.304	−0.090	−0.100	0.097	0.143
Transitivity	0.601	0.465	−0.137	−0.140	0.152	0.136
Modularity	0.046	0.136	0.090	−0.047	0.052	**0.004****
Measures of integration						
Characteristic path length	2.721	3.490	0.768	−0.691	0.600	**0.029***
Global efficiency	0.436	0.384	−0.052	−0.071	0.090	0.308
Measures of centrality						
Average degree	39.762	38.143	−1.619	−1.713	0.955	0.097
Average eccentricity	5.746	6.443	0.698	−1.115	1.017	0.274
Measures of resilience						
Assortativity coefficient	−0.074	−0.070	0.004	−0.034	0.028	0.739

Notes: Data are presented as the means. CI, 95% confidence interval of the difference between the groups. *$P < 0.05$; **$P < 0.01$; ***$P < 0.001$.

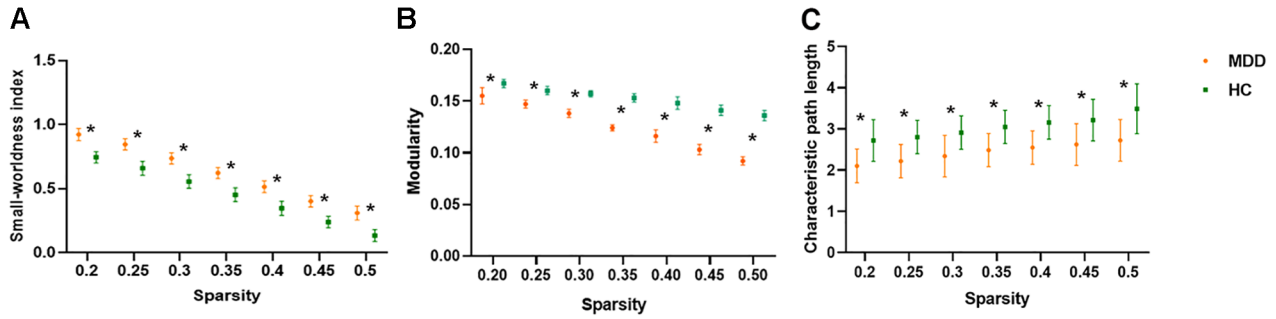

Figure 2: Small-worldness index (A), modularity (B), and characteristic path length (C) values of the patients with MDD and HCs at the network sparsity of 20–50% at intervals of 5%. ∗ represents significance between groups.

Decreased modularity suggests that the network examined could be less clearly separated into a collection of communities (Rubinov and Sporns, 2010). Together with higher network integration, our findings may suggest that patients with MDD had a less organized network structure within the hippocampus–amygdala anatomical network. An abnormal hippocampus–amygdala complex network could be the neuroanatomical basis disrupted feedback and/or feedforward systems between the hippocampus and amygdala, which in turn leads to dysregulated emotional memory that could contribute to MDD. Indeed, in animal models, activation of projections from the anterior basolateral amygdala nucleus to CA1 induces anxiety and social deficits, while activation of projections from the posterior basolateral amygdala nucleus to CA1 mediates learned hopeful or positive motivation in the face of pressure-facilitated spatial memory (Yang *et al.*, 2016; Yang and Wang, 2017). Hippocampus-dependent, episodic representation of emotionally significant content can influence the amygdala in functional MRI studies in human participants (Funayama *et al.*, 2001; Ochsner *et al.*, 2002; Schaefer *et al.*, 2002).

We found the small-worldness index is significantly different between patients with MDD and HCs. However, the small-worldness indexes in both groups were smaller than 1, indicating that the network within the hippocampus–amygdala complex does not preserve a small-world organization (Humphries and Gurney, 2008). As the small-worldness index is calculated as the proportion of the clustering coefficient and characteristic path length of the graph compared to random graphs and we found that the characteristic path length was significantly shorter in patients than in HCs; our finding of a significantly increased small-worldness index in patients with MDD is likely driven by a

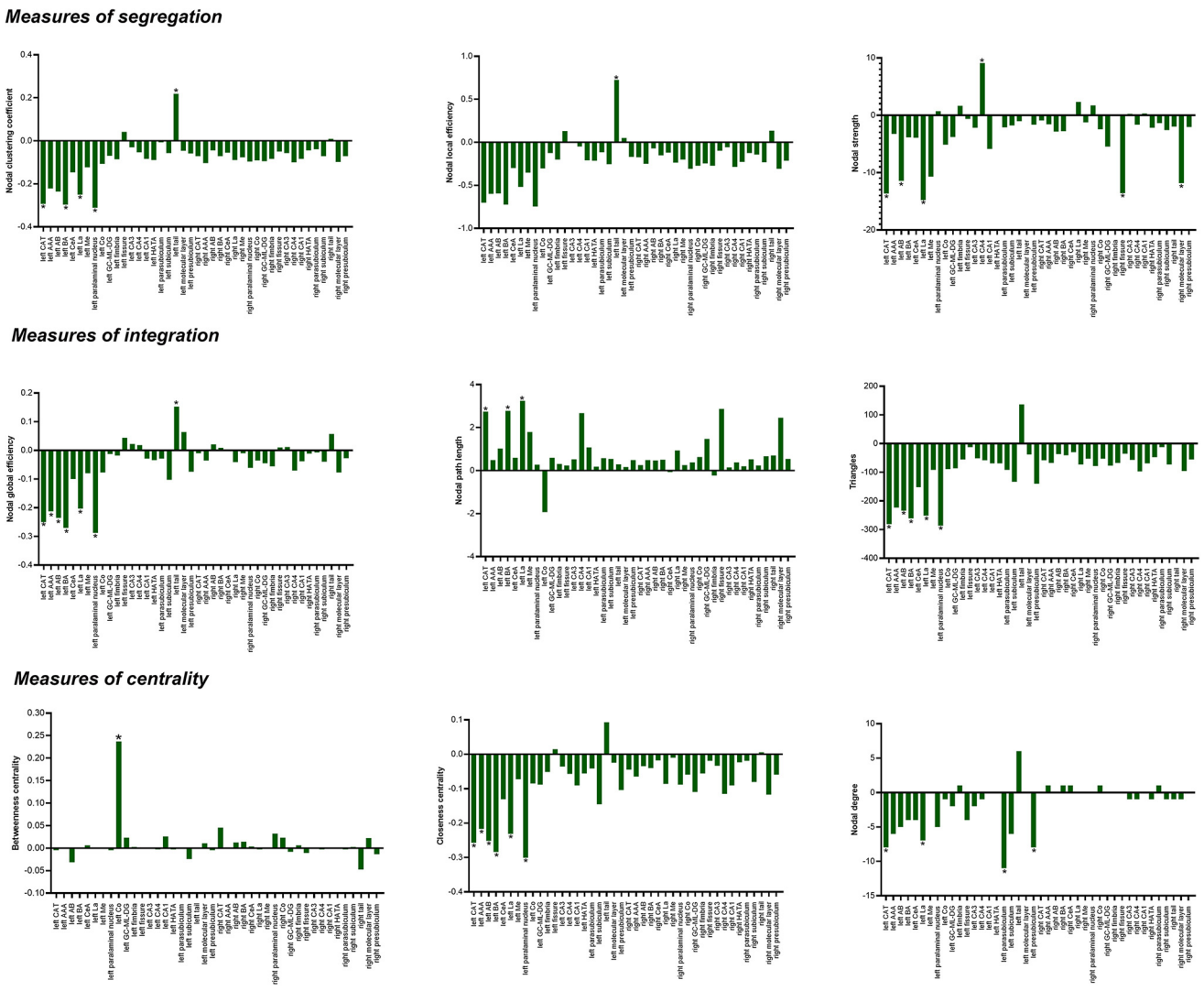

Figure 3: The group differences in the topological properties of each node within the SCN of the hippocampus–amygdala complex between MDD patients and HCs. Abbreviations: L, left; R, right; HATA, hippocampus–amygdala transition area; GC-ML-DG, granule cell and molecular layers of the dentate gyrus; CA, cornu ammonis. ∗ indicates FDR-corrected $P < 0.05$.

reduced characteristic path length in patients (Humphries and Gurney, 2008).

Analyses of nodal graph metrics highlights the distinct role of the left hippocampal tail in the hippocampus–amygdala complex. Specifically, the left hippocampal tail in patients with MDD showed higher measures of centrality (higher closeness centrality, clustering coefficient, degree, global/local efficiency, and triangles but lower path length), while other subfields/subregions showed an opposite direction of change when compared with HCs. These alterations in graph metrics indicate that the left hippocampal tail could be an abnormal hub in the hippocampus–amygdala network in patients with MDD. The hippocampal tail was previously shown to have anatomical differences in patients with MDD, and our study further identified its important role in the abnormal hippocampus–amygdala structural network related to MDD (Maller *et al.*, 2017; Nogovitsyn *et al.*, 2020). Anatomical evidence from rodents demonstrates that reciprocal connectivity between the amygdala and the hippocampus is largely confined to the ventral two-thirds (corresponding to the hippocampal head and tail), and a study reported that the dorsal-most portion of the hippocampus (corresponding to the hippocampal tail) does not innervate the amygdala (Pikkarainen *et al.*, 1999; Pitkänen *et al.*, 2000; Petrovich *et al.*, 2001). In primates, hippocampus–amygdala topographical projections are more restricted to the most anterior CA1 and presubiculum (Fudge *et al.*, 2012). SCNs do not necessarily correspond to white matter projections; however, they are more similar to patterns of functional connectivity than the architecture of white matter connections. Further studies are needed to clarify why and how the alteration pattern of SCN metrics in the hippocampal tail stands out from other subfields of the hippocampus or subregions of the amygdala.

Nodes within the left amygdala (except for the left Co) showed lower measures of centrality, significantly lower degree, closeness centrality, clustering coefficients, degree, triangle, strength and global/local efficiency, and longer path length. These findings suggested that subregions within the left amygdala were less connected with other nodes in the hippocampus–amygdala network. The amygdala shows significant lateralized activation during emotion processing, with more frequent activation on the left than on the right (Baas *et al.*, 2004). A previous study reported lower resting-state functional connectivity of the left amygdala with the cognitive control network in a population with

subthreshold depression (Peng *et al.*, 2020). Moreover, a study found that each individual with depression had lateralized amygdala activity, and the direction of asymmetry persisted even after treatment (Chen *et al.*, 2014). Our findings further demonstrated lateralized amygdala abnormalities in terms of topological characteristics within the hippocampus–amygdala complex.

There are certain limitations in the present study. First, our sample included only first-episode, comorbidity-free patients. While including this clinically homogeneous sample provides an advantage in identifying MDD-specific alterations unrelated to treatment and illness course, our result may not generalize to MDD patients with comorbid disorders or with a history of multiple episodes. Longitudinal studies and cross-sectional comparison studies are needed to resolve these factors. Second, we investigated the intrinsic SCN within the hippocampus–amygdala complex but could not locate anatomical projections or functional connectivity alterations. Further studies are warranted to determine the underlying biological mechanisms of topological changes within the hippocampus-amygdala network.

Conclusions

The current study presented the first evidence of atypical topological characteristics within the hippocampus–amygdala complex in patients with MDD using volumetric SCN analyses. The intrinsic hippocampus–amygdala network showed increased network integration but decreased segregation in patients with MDD compared to HCs. While the left hippocampal tail showed abnormally increased measures of centrality, nodes in the left amygdala showed reduced measures of centrality. These patterns of alteration may be a consequence of common neural substrates that influence multiple sites in the hippocampus and amygdala that underlying neuropathology of MDD. Future studies are needed to clarify the cause of altered topology, the affective/functional consequences of atypical topologic properties of the hippocampus–amygdala network that could contribute to the clinical presentation of MDD, and the degree to which the topologic properties are a risk factor for MDD or are reduced by antidepressant therapy over the course of illness.

Supplementary Data

Supplementary data are available at *Psychoradiology* online.

Data Availability Statement

The datasets generated during and/or analyzed during the current study are not publicly available due as participants did not consent to public release but are available from the corresponding author on reasonable request.

Author Contributions

L.Z., X.H., W.K., and W.J. are responsible for the conception and design of the study. M.T., Q.H., and Z.Z. were responsible for the acquisition of data. L.Z. and X.H. supervised the technical settings for MRI and FreeSurfer. L.Z., X.H., Y.H., Y.G., and H.L. were constantly involved in the analysis and interpretation of data. All authors substantively wrote and revised the manuscript and approved the final manuscript.

Conflict of Interest

The authors declare no conflicts of interest.

Acknowledgements

This study is supported by grants from 1.3.5 Project for Disciplines of Excellence, West China Hospital, Sichuan University (ZYJC21041), The Research Project of Shanghai Science and Technology Commission (20dz2260300), and The Fundamental Research Funds for the Central Universities.

References

Achard S, Bullmore E (2007) Efficiency and cost of economical brain functional networks. *PLoS Comput Biol* **3**:e17.

Amaral LA, Scala A, Barthelemy M, *et al.* (2000) Classes of small-world networks. *Proc Natl Acad Sci U S A* **97**:11149–52.

Baas D, Aleman A, Kahn RS (2004) Lateralization of amygdala activation: a systematic review of functional neuroimaging studies. *Brain Res Rev* **45**:96–103.

Barrat A, Barthélemy M, Pastor-Satorras R, *et al.* (2004) The architecture of complex weighted networks. *Proc Natl Acad Sci U S A* **101**:3747–52.

Bassett DS, Bullmore E (2006) Small-world brain networks. *Neuroscientist* **12**:512–23.

Boll S, Gamer M, Gluth S, *et al.* (2013) Separate amygdala subregions signal surprise and predictiveness during associative fear learning in humans. *Eur J Neurosci* **37**:758–67.

Brandes U (2001) A faster algorithm for betweenness centrality. *J Math Sociol* **25**:163–77.

Chen T, Kendrick KM, Wang J, *et al.* (2017) Anomalous single-subject based morphological cortical networks in drug-naive, first-episode major depressive disorder. *Hum Brain Mapp* **38**:2482–94.

Chen YT, Huang MW, Hung IC, *et al.* (2014) Right and left amygdalae activation in patients with major depression receiving antidepressant treatment, as revealed by fMRI. *Behav Brain Funct* **10**:36.

Chen Z, Huang X, Gong Q, *et al.* (2021) Translational application of neuroimaging in major depressive disorder: a review of psychoradiological studies. *Front Med* **15**:528–40.

Fischl B, Salat DH, Busa E, *et al.* (2002) Whole brain segmentation: automated labeling of neuroanatomical structures in the human brain. *Neuron* **33**:341–55.

Freeman LC (1978) Centrality in social networks conceptual clarification. *Social Networks* **1**:215–39.

Fudge JL, deCampo DM, Becoats KT (2012) Revisiting the hippocampal-amygdala pathway in primates: association with immature-appearing neurons. *Neuroscience* **212**:104–19.

Funayama ES, Grillon C, Davis M, *et al.* (2001) A double dissociation in the affective modulation of startle in humans: effects of unilateral temporal lobectomy. *J Cogn Neurosci* **13**:721–9.

Han S, Zheng R, Li S, *et al.* (2022) Resolving heterogeneity in depression using individualized structural covariance network analysis. *Psychol Med* 1–10.

Harris J, Hirst JL, Mossinghoff M (2008) *Combinatorics and Graph Theory*, Springer.

Ho TC, Gutman B, Pozzi E, *et al.* (2022) Subcortical shape alterations in major depressive disorder: findings from the ENIGMA major depressive disorder working group. *Hum Brain Mapp* **43**:341–51.

Hu X, Zhang L, Hu X, *et al.* (2019) Abnormal hippocampal subfields may Be potential predictors of worse early response to

antidepressant treatment in drug-Naïve patients with major depressive disorder. *J Magn Reson Imaging* **49**:1760–8.
Humphries MD, Gurney K (2008) Network 'small-world-ness': a quantitative method for determining canonical network equivalence. *PLoS One* **3**:e0002051.
Iglesias JE, Augustinack JC, Nguyen K, *et al.* (2015) A computational atlas of the hippocampal formation using ex vivo, ultra-high resolution MRI: application to adaptive segmentation of in vivo MRI. *Neuroimage* **115**:117–37.
Kim H, Han KM, Choi KW, *et al.* (2021) Volumetric alterations in subregions of the amygdala in adults with major depressive disorder. *J Affect Disord* **295**:108–15.
Latora V, Marchiori M (2001) Efficient behavior of small-world networks. *Phys Rev Lett* **87**:198701.
Li X, Cao Q, Pu F, *et al.* (2015) Abnormalities of structural covariance networks in drug-naïve boys with attention deficit hyperactivity disorder. *Psychiatry Res* **231**:273–8.
Li Y, Chu T, Che K, *et al.* (2021) Altered gray matter structural covariance networks in postpartum depression: a graph theoretical analysis. *J Affect Disord* **293**:159–67.
Liu J, Xu X, Zhu C, *et al.* (2020) Disrupted structural brain network organization behind depressive symptoms in major depressive disorder. *Front Psychiatry* **11**:565890.
Liu Z, Palaniyappan L, Wu X, *et al.* (2021) Resolving heterogeneity in schizophrenia through a novel systems approach to brain structure: individualized structural covariance network analysis. *Mol Psychiatry* **26**:7719–31.
Maller JJ, Broadhouse K, Rush AJ, *et al.* (2017) Increased hippocampal tail volume predicts depression status and remission to anti-depressant medications in major depression. *Mol Psychiatry* **23**:1737–44.
Mijalkov M, Kakaei E, Pereira JB, *et al.* (2017) BRAPH: a graph theory software for the analysis of brain connectivity. *PLoS One* **12**:e0178798.
Newman ME (2002) Assortative mixing in networks. *Phys Rev Lett* **89**:208701.
Newman MEJ (2003) The structure and function of complex networks. *SIAM Rev* **45**:167–256.
Newman MEJ (2006) Modularity and community structure in networks. *Proc Natl Acad Sci USA* **103**:8577–82.
Nogovitsyn N, Muller M, Souza R, *et al.* (2020) Hippocampal tail volume as a predictive biomarker of antidepressant treatment outcomes in patients with major depressive disorder: a CAN-BIND report. *Neuropsychopharmacology* **45**:283–91.
Ochsner KN, Bunge SA, Gross JJ, *et al.* (2002) Rethinking feelings: an FMRI study of the cognitive regulation of emotion. *J Cogn Neurosci* **14**:1215–29.
Onnela JP, Saramäki J, Kertész J, *et al.* (2005) Intensity and coherence of motifs in weighted complex networks. *Phys Rev E Stat Nonlin Soft Matter Phys* **71**:065103.
Otte C, Gold SM, Penninx BW, *et al.* (2016) Major depressive disorder. *Nat Rev Dis Primers* **2**:16065.
Peng X, Lau WKW, Wang C, *et al.* (2020) Impaired left amygdala resting state functional connectivity in subthreshold depression individuals. *Sci Rep* **10**:17207.
Petrovich GD, Canteras NS, Swanson LW (2001) Combinatorial amygdalar inputs to hippocampal domains and hypothalamic behavior systems. *Brain Res Rev* **38**:247–89.
Pikkarainen M, Rönkkö S, Savander V, *et al.* (1999) Projections from the lateral, basal, and accessory basal nuclei of the amygdala to the hippocampal formation in rat. *J Comp Neurol* **403**:229–60.
Pitkänen A, Pikkarainen M, Nurminen N, *et al.* (2000) Reciprocal connections between the amygdala and the hippocampal formation, perirhinal cortex, and postrhinal cortex in rat. A review. *Ann NY Acad Sci* **911**:369–91.
Plachti A, Kharabian S, Eickhoff SB, *et al.* (2020) Hippocampus coatrophy pattern in dementia deviates from covariance patterns across the lifespan. *Brain* **143**:2788–802.
Qi T, Schaadt G, Cafiero R, *et al.* (2019) The emergence of long-range language network structural covariance and language abilities. *Neuroimage* **191**:36–48.
Reuter M, Rosas HD, Fischl B (2010) Highly accurate inverse consistent registration: a robust approach. *Neuroimage* **53**:1181–96.
Roddy D, Kelly JR, Farrell C, *et al.* (2021) Amygdala substructure volumes in Major Depressive Disorder. *Neuroimage Clin* **31**:102781.
Rubinov M, Sporns O (2010) Complex network measures of brain connectivity: uses and interpretations. *Neuroimage* **52**:1059–69.
Saygin ZM, Kliemann D, Iglesias JE, *et al.* (2017) High-resolution magnetic resonance imaging reveals nuclei of the human amygdala: manual segmentation to automatic atlas. *Neuroimage* **155**:370–82.
Schaefer SM, Jackson DC, Davidson RJ, *et al.* (2002) Modulation of amygdalar activity by the conscious regulation of negative emotion. *J Cogn Neurosci* **14**:913–21.
Schmaal L, Veltman DJ, van Erp TG, *et al.* (2016) Subcortical brain alterations in major depressive disorder: findings from the ENIGMA Major Depressive Disorder working group. *Mol Psychiatry* **21**:806–12.
Sled JG, Zijdenbos AP, Evans AC (1998) A nonparametric method for automatic correction of intensity nonuniformity in MRI data. *IEEE Trans Med Imaging* **17**:87–97.
Terranova JI, Yokose J, Osanai H, *et al.* (2022) Hippocampal-amygdala memory circuits govern experience-dependent observational fear. *Neuron* **110**:1416–31.e13.
Watanabe K, Kakeda S, Katsuki A, *et al.* (2020) Whole-brain structural covariance network abnormality in first-episode and drug-naïve major depressive disorder. *Psychiatry Res Neuroimaging* **300**:111083.
Watts DJ, Strogatz SH (1998) Collective dynamics of 'small-world' networks. *Nature* **393**:440–2.
Weissman DG, Lambert HK, Rodman AM, *et al.* (2020) Reduced hippocampal and amygdala volume as a mechanism underlying stress sensitization to depression following childhood trauma. *Depress Anxiety* **37**:916–25.
Whelan CD, Hibar DP, van Velzen LS, *et al.* (2016) Heritability and reliability of automatically segmented human hippocampal formation subregions. *Neuroimage* **128**:125–37.
Xiong G, Dong D, Cheng C, *et al.* (2021) Potential structural trait markers of depression in the form of alterations in the structures of subcortical nuclei and structural covariance network properties. *Neuroimage Clin* **32**:102871.
Yang Y, Wang JZ (2017) From structure to behavior in basolateral amygdala-Hippocampus circuits. *Front Neural Circuits* **11**:86.
Yang Y, Wang ZH, Jin S, *et al.* (2016) Opposite monosynaptic scaling of BLP-vCA1 inputs governs hopefulness- and helplessness-modulated spatial learning and memory. *Nat Commun* **7**:11935.
Yao Z, Fu Y, Wu J, *et al.* (2020) Morphological changes in subregions of hippocampus and amygdala in major depressive disorder patients. *Brain Imaging Behav* **14**:653–67.
Ye M, Yang T, Qing P, *et al.* (2015) Changes of functional brain networks in major depressive disorder: a graph theoretical analysis of resting-state fMRI. *PLoS ONE* **10**:e0133775.
Yee Y, Fernandes DJ, French L, *et al.* (2018) Structural covariance of brain region volumes is associated with both structural connectivity and transcriptomic similarity. *Neuroimage* **179**:357–72.
Yu Z, Qin J, Xiong X, *et al.* (2020) Abnormal topology of brain functional networks in unipolar depression and bipolar disorder using

optimal graph thresholding. *Prog Neuropsychopharmacol Biol Psychiatry* **96**:109758.

Yun JY, Boedhoe PSW, Vriend C, *et al.* (2020) Brain structural covariance networks in obsessive-compulsive disorder: a graph analysis from the ENIGMA Consortium. *Brain* **143**: 684–700.

Zavorotnyy M, Zöllner R, Schulte-Güstenberg LR, *et al.* (2018) Low left amygdala volume is associated with a longer duration of unipolar depression. *J Neural Transm (Vienna)* **125**:229–38.

Zielinski BA, Gennatas ED, Zhou J, *et al.* (2010) Network-level structural covariance in the developing brain. *Proc Natl Acad Sci U S A* **107**:18191–6.